Synthesis and Crystal Structures of New Lanthanide Hydroxyhalide Anion Exchange Materials, $Ln_2(OH)_5X \cdot 1.5H_2O$ (X = Cl, Br; Ln = Y, Dy, Er, Yb)

Leslie Poudret,[†] Timothy J. Prior,[‡] Laura J. McIntyre,[†] and Andrew M. Fogg[†,*]

Department of Chemistry, University of Liverpool, Liverpool L69 7ZD, United Kingdom, and Department of Chemistry, University of Hull, Kingston upon Hull HU6 7RX, United Kingdom

Received August 26, 2008. Revised Manuscript Received October 17, 2008

A family of layered lanthanide hydroxyhalide intercalation hosts, $Ln_2(OH)_5X \cdot 1.5H_2O$ (X = Cl, Br; Ln = Y, Dy, Er, Yb), has been synthesized under hydrothermal conditions and their crystal structure determined. These are the first structures for the $m = 1$ members of the $Ln_2(OH)_{6-m}(A)_m \cdot nH_2O$ family of intercalation hosts to be determined. Reaction mixtures with Ln = Yb always yield a biphasic product which adopts an orthorhombic or monoclinic crystal structure. In both cases the layer composition is $[Yb_2(OH)_5(H_2O)_{1.5}]^+$ and the Yb is eight or nine coordinated to bridging hydroxide anions and coordinated water molecules. Charge balancing halide anions are located in the interlayer gallery. The orthorhombic structure is adopted by the other chloride host lattices and the monoclinic one by $Y_2(OH)_5Br \cdot 1.5H_2O$. These materials have been shown to undergo facile room temperature anion exchange reactions with a range of organic dicarboxylates.

Introduction

Anion exchange materials, particularly those based on metal hydroxide layers, have become well-known as a result of having found numerous applications in fields including catalysis,[1,2] separation technology,[3−5] and pharmaceuticals.[6−9] This diversity of applications is a consequence of the compositional flexibility of this class of materials where both the identity of the metal cation within the layer and the interlayer anion can be controlled to target a specific application. A recent review by Feng and Duan details the technological importance of layered double hydroxides (LDHs).[10] The LDHs are the most widely studied family of layered hydroxides and can be divided into two distinct groups, those related to brucite ($Mg(OH)_2$) and those derived from gibbsite (γ-$Al(OH)_3$). The former are the larger family and have the general formula $[M^{2+}_{1-y}M^{3+}_{y}(OH)_2]^{y+}$-$X^{m-}_{y/m} \cdot nH_2O$ (e.g., M^{2+} = Mg, Zn, Co, Ni; M^{3+} = Al, Cr, Fe, Ga) and typically, they are synthesized with nitrate or chloride as the charge balancing, exchangeable anion.[1,11,12] LDHs can also be prepared from gibbsite, or the other $Al(OH)_3$ polymorphs, by intercalation of lithium salts[13−16] or $M(NO_3)_2$ (M = Co, Ni, Cu, or Zn)[17−19] into the structure with the metal cation occupying the vacant octahedral sites within the $Al(OH)_3$ layer with the anion located between the layers.

Other families of anion exchange materials include the hydroxy double salts (HDSs) and hydroxynitrates. The HDSs differ from the LDHs in that they contain two divalent metal cations within the layers giving the general formulas $(M^{2+}Me^{2+})_5(OH)_8(X^{m-})_{2/m}$ and $[(M^{2+}_{1-y}Me^{2+}_{1+y})(OH)_{3(1-z)}]^+$-$X^{m-}_{(1+3z)/m}$. In these materials the compositional diversity is greatly reduced in comparison to the layered double hydroxides with the metal cations being limited to M^{2+} = Ni^{2+}, Co^{2+} or Zn^{2+} which are octahedrally coordinated and Me^{2+} = Cu^{2+} or Zn^{2+} which occupy tetrahedral sites above and below the vacant octahedral sites within the layer.[20−23]

Hydroxynitrate phases, $Ln_2(OH)_{6-m}(NO_3)_m \cdot nH_2O$, are known for the lanthanide cations. A variety of phases of

* To whom all correspondence should be addressed. Tel: 44 151 794 2047. Fax: 44 151 794 3587. E-mail: afogg@liverpool.ac.uk.
[†] University of Liverpool.
[‡] University of Hull.

(1) Cavani, F.; Trifiro, F.; Vaccari, A. *Catal. Today* **1991**, *11*, 173.
(2) Sels, B. F.; De Vos, D. E.; Jacobs, P. A. *Catal. Rev. Sci. Eng.* **2001**, *43*, 443.
(3) Fogg, A. M.; Dunn, J. S.; Shyu, S. G.; Cary, D. R.; O'Hare, D. *Chem. Mater.* **1998**, *10*, 351.
(4) Fogg, A. M.; Green, V. M.; Harvey, H. G.; O'Hare, D. *Adv. Mater.* **1999**, *11*, 1466.
(5) Ragavan, A.; Khan, A.; O'Hare, D. *J. Mater. Chem.* **2006**, *16*, 4155.
(6) Choy, J. H.; Jung, J. S.; Oh, J. M.; Park, M.; Jeong, J.; Kang, Y. K.; Han, O. J. *Biomaterials* **2004**, *25*, 3059.
(7) Li, B. X.; He, J.; Evans, D. G.; Duan, X. *Appl. Clay Sci.* **2004**, *27*, 199.
(8) Ambrogi, V.; Fardella, G.; Grandolini, G.; Perioli, L. *Int. J. Pharm.* **2001**, *220*, 23.
(9) Khan, A. I.; Lei, L. X.; Norquist, A. J.; O'Hare, D. *Chem. Commun.* **2001**, 2342.
(10) Feng, L.; Duan, X. *Struct. Bonding* **2006**, *119*, 193.
(11) Khan, A. I.; O'Hare, D. *J. Mater. Chem.* **2002**, *12*, 3191.
(12) Williams, G. R.; O'Hare, D. *J. Mater. Chem.* **2006**, *16*, 3065.
(13) Besserguenev, A. V.; Fogg, A. M.; Francis, R. J.; Price, S. J.; OHare, D.; Isupov, V. P.; Tolochko, B. P. *Chem. Mater.* **1997**, *9*, 241.
(14) Fogg, A. M.; Freij, A. J.; Parkinson, G. M. *Chem. Mater.* **2002**, *14*, 232.
(15) Fogg, A. M.; O'Hare, D. *Chem. Mater.* **1999**, *11*, 1771.
(16) Poeppelmeier, K. R.; Hwu, S. J. *Inorg. Chem.* **1987**, *26*, 3297.
(17) Fogg, A. M.; Williams, G. R.; Chester, R.; O'Hare, D. *J. Mater. Chem.* **2004**, *14*, 2369.
(18) Williams, G. R.; Dunbar, T. G.; Beer, A. J.; Fogg, A. M.; O'Hare, D. *J. Mater. Chem.* **2006**, *16*, 1231.
(19) Williams, G. R.; Dunbar, T. G.; Beer, A. J.; Fogg, A. M.; O'Hare, D. *J. Mater. Chem.* **2006**, *16*, 1222.
(20) Kandare, E.; Hossenlopp, J. M. *J. Phys. Chem. B* **2005**, *109*, 8469.
(21) Kasai, A.; Fujihara, S. *Inorg. Chem.* **2006**, *45*, 415.
(22) Meyn, M.; Beneke, K.; Lagaly, G. *Inorg. Chem.* **1993**, *32*, 1209.

10.1021/cm802301a CCC: $40.75
Published on Web 11/17/2008

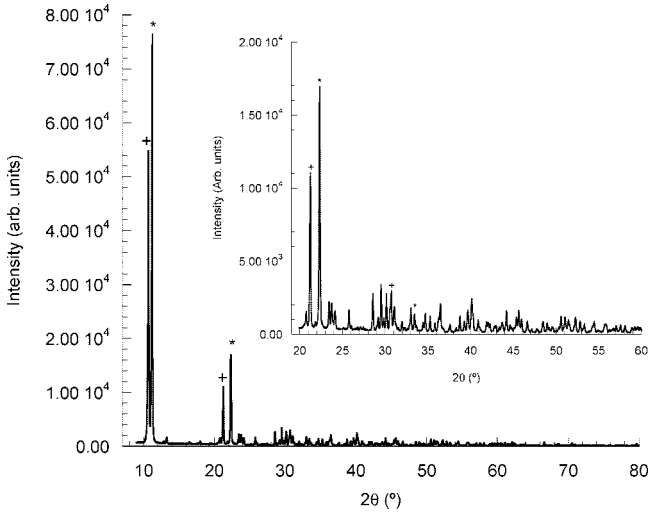

Figure 1. Powder X-ray diffraction pattern of $Yb_2(OH)_5Cl\cdot 1.5H_2O$ showing two layered phases with interlayer separations of 8.03 Å and 8.42 Å. INSET: Enlarged diffraction pattern covering the 2θ range 20−60°. * indicates the reflections corresponding to the interlayer separation of the 8.0 Å phase and + those of the 8.4 Å phase.

varying hydration with $m = 1$ have been reported. Anion exchangeable $Ln_2(OH)_5(NO_3)\cdot 1.5H_2O$ (Ln = Y, Gd−Lu) phases have recently been reported for the smaller lanthanides, with exchange being demonstrated by reaction with a range of organic carboxylate and sulfonate anions.[24,25] The synthesis of materials with a higher degree of hydration, $Ln_2(OH)_5(NO_3)\cdot 2H_2O$, has been reported for Ln = Y and Yb although anion exchange has not been demonstrated for these phases.[26−28] Materials in the $m = 2$ family with the composition $Ln(OH)_2NO_3\cdot nH_2O$ (Ln = La, Pr, Nd, Sm−Dy; $n = 0, 1$) have been synthesized with the larger lanthanide cations.[29−32] These materials differ structurally from the others as the nitrate anion is coordinated to the lanthanide cation rather than being located in the interlayer gallery. This, however, has not prevented anion exchange reactions being observed between $La(OH)_2NO_3\cdot H_2O$ and acetate, benzoate, and terephthalate.[33]

Anhydrous lanthanide hydroxychloride materials, $Ln(OH)_2Cl$ are also known for Ln = Y, La, Nd, Sm, and Gd.[34−39] These materials are polymorphic, having monoclinic and orthorhombic structures, in which the chloride is located between the $Ln(OH)_2^+$ layers. There have been no previous reports of anion exchange with the $Ln(OH)_2Cl$ materials or of the $m = 1$ members of the family, $Ln_2(OH)_5Cl\cdot nH_2O$. In this paper, we report the synthesis and crystal structures of new lanthanide hydroxyhalide phases, $Ln_2(OH)_5X\cdot 1.5H_2O$ (X = Cl, Br; Ln = Y, Dy, Er, and Yb) and describe their anion exchange chemistry.

Table 1. Summary of the Crystallographic Information for the Monoclinic and Orthorhombic Polymorphs of $Yb_2(OH)_5Cl\cdot 1.5H_2O$

	8.4 Å phase	8 Å phase
empirical formula	$Cl_2O_{13}Yb_4$	$Cl_2O_{13}Yb_4$
fw	971.06	971.06
T (K)	120(2)	120(2)
wavelength (Å)	0.69430	0.69430
cryst syst	orthorhombic	monoclinic
space group	$Pca2_1$ (No. 29)	$P2_1$ (No. 4)
a (Å)	12.5108(10)	7.0245(7)
b (Å	8.3930(13)	12.5199(12)
c (Å	7.0438(10)	8.3174(8)
α, β, γ/°	90, 90, 90	90, 105.9750(10), 90
V (Å^3)	739.62(17)	703.23(12)
Z	2	2
density (calculated) (Mg m^{-3})	4.360	4.586
absorp coeff (mm^{-1})	25.467	26.784
$F(000)$	836	836
cryst size (mm^3)	0.08 × 0.01 × 0.01	0.05 × 0.04 × 0.005
θ range for data collection (deg)	2.85 to 30.85	2.95 to 31.07
index ranges	$-18 \le h \le 18$, $-12 \le k \le 12$, $-10 \le l \le 10$	$-10 \le h \le 10$, $-17 \le k \le 18$, $-12 \le l \le 12$
no. of reflns collected	7946	8202
no. of independent reflns, R_{int}	1277, 0.0328	4201, 0.0390
completeness to $\theta = 26.00°$ (%)	98.7	99.5
absorp corr	semiempirical from equivalents	semiempirical from equivalents
max. and min. transmission	1.00 and 0.7242	0.875 and 0.276
refinement method	full-matrix least-squares on F^2	full-matrix least-squares on F^2
data/restraints/params	1277/43/91	4201/79/173
GOF on F^2	1.178	1.027
final R indices [$I > 2\sigma(I)$]	$R_1 = 0.0330$, $wR_2 = 0.0685$	$R_1 = 0.0307$, $wR_2 = 0.0661$
R indices (all data)	$R_1 = 0.0410$, $wR_2 = 0.0733$	$R_1 = 0.0330$, $wR_2 = 0.0675$
absolute structure param	−0.02(5)	0.33(2)
largest diff. peak and hole (e Å^{-3})	2.872 and −4.889	1.694 and −1.690

Experimental Section

Synthesis. All of the anion exchange host lattices described in this paper were prepared via a hydrothermal synthesis. Typically, 7.5 mL of a 0.44 M aqueous solution of $LnX_3\cdot nH_2O$ (X = Cl, Br; Ln = Y, La, Ce, Nd, Dy, Er or Yb) was added to 2.5 mL of an aqueous solution containing 2.1 M NaOH and 1.44 M NaX (X = Cl, Br). A gelatinous precipitate was formed instantaneously and the resulting mixture was treated hydrothermally at 150 °C for 12 h. The resulting product was then filtered, washed with deionized water and ethanol before being dried in air at room temperature.

(23) Stahlin, W.; Oswald, H. R. *Acta Crystallogr., Sect. B* **1970**, *B 26*, 860.
(24) McIntyre, L. J.; Jackson, L. K.; Fogg, A. M. *J. Phys. Chem. Solids* **2008**, *69*, 1070.
(25) McIntyre, L. J.; Jackson, L. K.; Fogg, A. M. *Chem. Mater.* **2008**, *20*, 335.
(26) Haschke, J. M. *Inorg. Chem.* **1974**, *13*, 1812.
(27) Holcombe, C. E. *J. Am. Ceram. Soc.* **1978**, *61*, 481.
(28) Schildermans, I.; Mullens, J.; Yperman, J.; Franco, D.; Vanpoucke, L. C. *Thermochim. Acta* **1994**, *231*, 185.
(29) Louer, D.; Louer, M. *J. Solid State Chem.* **1987**, *68*, 292.
(30) Louer, M.; Louer, D.; Delgado, A. L.; Martinez, O. G. *Eur. J. Solid State Inorg. Chem* **1989**, *26*, 241.
(31) Lundberg, M.; Skarnulis, A. J. *Acta Crystallogr., Sect. B* **1976**, *32*, 2944.
(32) Mullica, D. F.; Sappenfield, E. L.; Grossie, D. A. *J. Solid State Chem.* **1986**, *63*, 231.
(33) Newman, S. P.; Jones, W. *J. Solid State Chem.* **1999**, *148*, 26.
(34) Bukin, V. I. *Dokl. Akad. Nauk SSSR* **1972**, *207*, 1332.
(35) Carter, F. L.; Levinson, S. *Inorg. Chem.* **1969**, *8*, 2788.
(36) Dornberger-Schiff, K.; Klevtsova, R. F. *Acta Crystallogr.* **1967**, *22*, 435.
(37) Jouve, C.; Marrot, J.; Riou, D. *Acta Crystallogr., Sect. C* **2002**, *58*, i14.
(38) Klevtsova, R. F.; Glinskaya, L. A. *Z. Strukt. Khim.* **1969**, *10*, 494.
(39) Tarkhova, T. N.; Grishin, I. A.; Mironov, N. N. *Zh. Neorg. Khim.* **1970**, *15*, 1340.

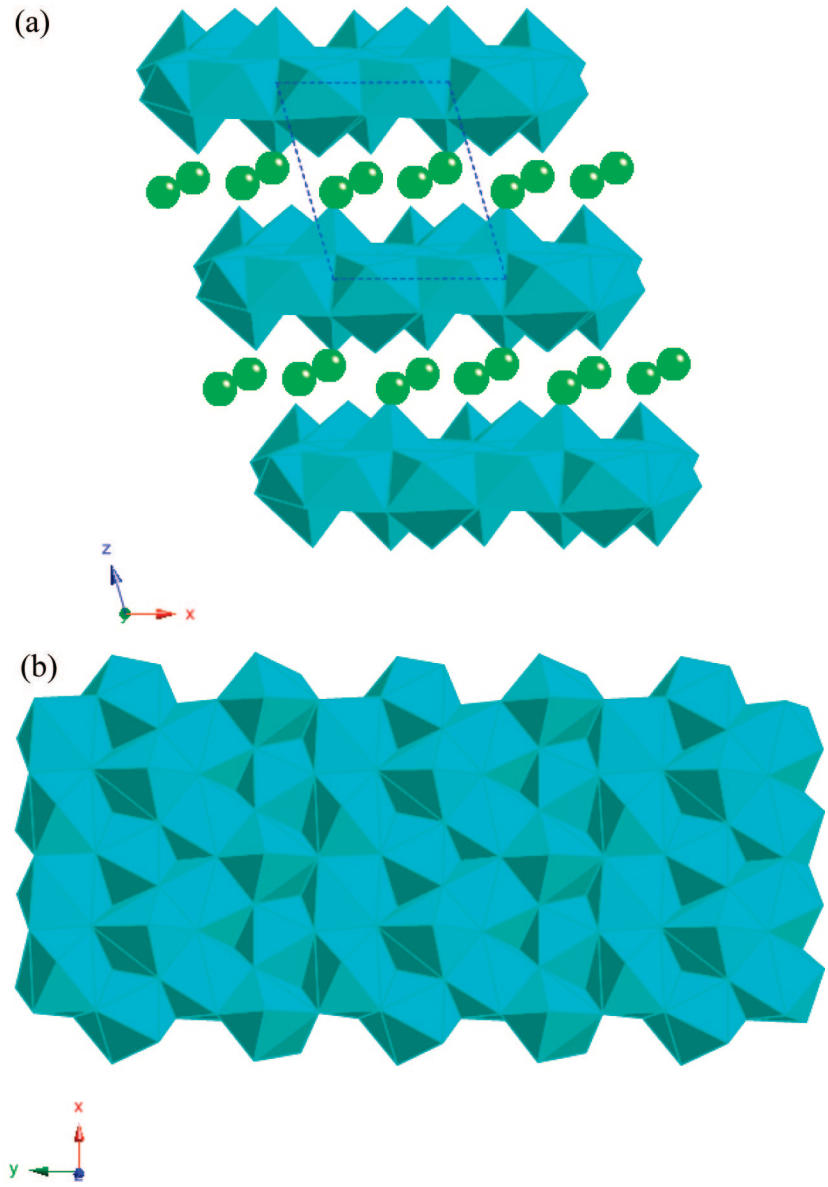

Figure 2. (a) Crystal structure and (b) layer structure of the 8.0 Å phase of $Yb_2(OH)_5Cl\cdot 1.5H_2O$.

Anion exchange reactions were performed between the $Ln_2(OH)_5X\cdot 1.5H_2O$ (X = Cl, Br; Ln = Y, Dy, Er, Yb) phases and a 3-fold molar excess of the following anions in aqueous solution: maleate, phthalate, terephthalate, and succinate. In each case, the reaction mixture was stirred at room temperature overnight before being filtered, washed with deionized water and ethanol, and left to dry in air.

Characterization. Powder X-ray diffraction patterns were recorded with Cu $K\alpha_1$ radiation on a Stoe Stadi-P diffractometer in either Bragg−Brentano or Debye−Scherrer geometry. A combination of thermogravimetric analysis (TGA) and elemental analysis was used to determine the stoichiometry of the materials. TGA traces were recorded on a Seiko SII-TG/DTA 6300 thermal analyzer. ICP analysis, to determine the metal content of the samples, was carried out on a Ciros CCD optical emission spectrometer following complete dissolution of the samples in dilute HNO_3 and CHN analysis was performed on a FlashEA 1112 instrument. Fourier transform infrared (FTIR) spectra were recorded on a Nicolet Nexus FT-IR spectrophotometer. For these measurements the samples (approximately 10 wt %) were mixed with KBr and pressed into a sample holder.

Single-crystal X-ray diffraction data were collected on the microcrystal diffraction facility of Station 9.8 at the UK Synchrotron Radiation Source, STFC Daresbury Laboratory. Crystals were covered in a thin film of perfluoropolyether oil and mounted at the end of a two-stage glass fiber and cooled in an Oxford Instruments nitrogen gas cryostream to 120 K. Data were collected using a Bruker D8 diffractometer operating with an APEXII CCD area-detector. Data collection nominally covered a sphere of reciprocal space in three series of ω-rotation exposure frames with different crystal orientation φ angles. Reflection intensities were integrated using standard procedures, allowing for the plane polarized nature of the primary synchrotron beam. Semiempirical corrections were applied to account for absorption and incident beam decay. Unit-cell parameters were refined using all observed reflections in the complete data sets.

Structures were solved by routine automatic direct methods. The structures were completed by least-squares refinement based on all unique measured F^2 values and difference Fourier methods.

Results and Discussion

New anion exchange hosts with the composition $Ln_2(OH)_5X\cdot 1.5H_2O$ (X = Cl, Br; Ln = Y, Dy, Er, Yb) have

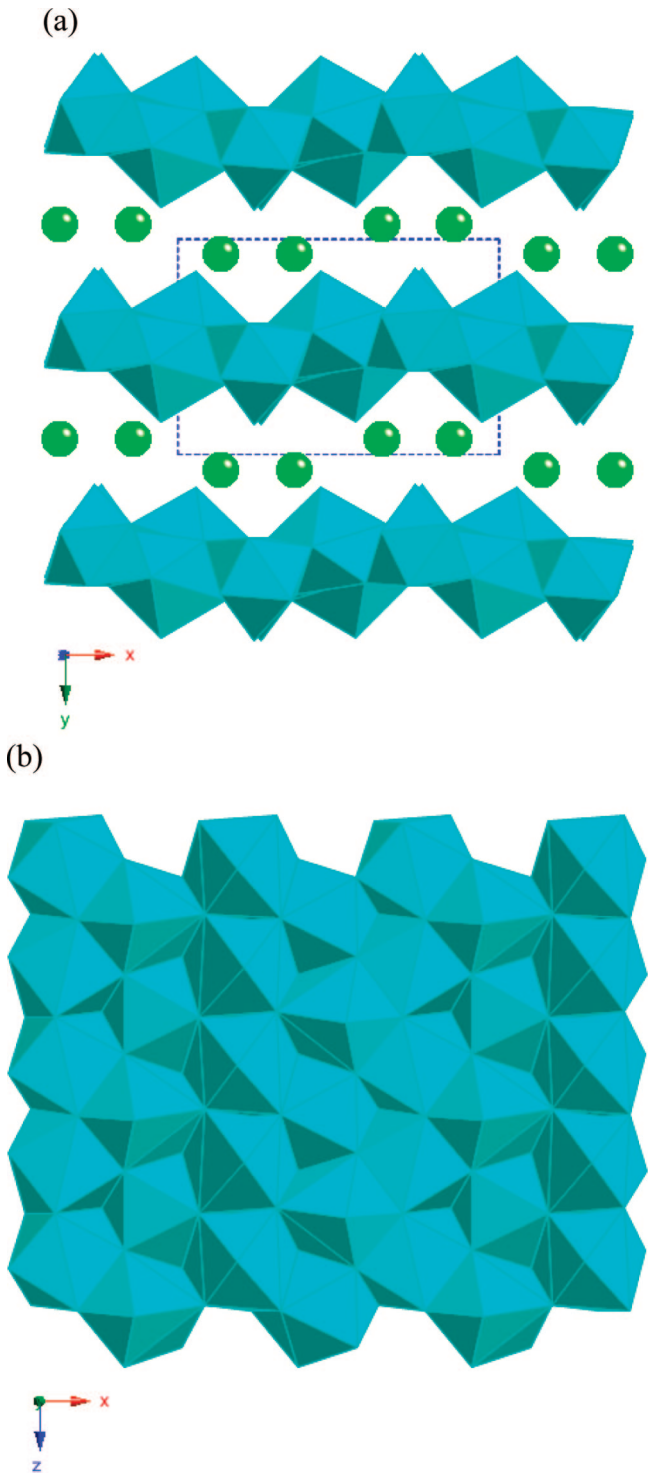

Figure 3. (a) Crystal structure and (b) layer structure of the 8.4 Å phase of $Yb_2(OH)_5Cl\cdot 1.5H_2O$.

been synthesized via a hydrothermal route. It was found that the Y, Dy, and Er phases were prepared pure while the Yb material was always biphasic despite extensive screening of the reaction variables through control of the reagent concentrations and temperature. Reactions with the larger lanthanides, La, Ce, and Nd, under the same conditions yielded the previously reported $Ln(OH)_2Cl$ phases.

The majority of the samples comprised microcrystalline powders, however, extremely small single crystals of both phases in the $Yb_2(OH)_5Cl\cdot 1.5H_2O$ sample were obtained. The powder X-ray diffraction pattern of $Yb_2(OH)_5Cl.1.5H_2O$ is given in Figure 1 and clearly shows the presence of two layered phases with interlayer separations of 8.0 Å, and 8.4 Å with the larger separation corresponding to the phase observed with Y, Dy, and Er.

The "8 Å phase" crystallizes in the noncentrosymmetric monoclinic space group $P2_1$. Full crystallographic details are given in Table 1 and the structure is illustrated in Figure 2. The asymmetric unit contains four independent Yb ions and has the formula $Yb_4(OH)_{10}(H_2O)_3Cl_2$. The Yb and hydroxide ions assemble into dense positively charged layers of composition $[Yb_2(OH)_5(H_2O)_{1.5}]^+$ formed of eight or nine coordinate Yb with each hydroxide bridging between three Yb ions. Each Yb is bound to a large number of hydroxide ions: Yb1 and Yb4 each bind to eight hydroxide ions, while Yb2 and Yb3 bind to seven. Yb−OH distances lie in the range 2.222 to 2.522 Å. In addition to the hydroxide, water is also bound to Yb1, Yb2, and Yb3 and projects perpendicular to the layer at distances between 2.363 and 2.521 Å. The Yb cations can be considered to be arranged in rows along *a*. A bound water projects into the interlayer region from three-quarters of these rows; with a water absent from every fourth row. The layers are related by the 2_1 screw axis and stacked perpendicular to the *ac* plane at a separation $c\sin\beta$ (7.996(3) Å). This is slightly larger than those typically seen in the LDHs reflecting the thicker, buckled layers in this material.[13] Adjacent layers are displaced by 2.288(8) Å so they do not overlie (see Figure 2a). Located in the interlayer region are charge-balancing chloride anions which form hydrogen bonds to hydroxide and water of the layers. For Cl1, three short hydrogen bonding contacts are identified and these lie in the range 3.10 to 3.26 Å (O···Cl distances). For Cl2, five short contacts are identified in the range 3.07−3.26 Å (O···Cl distances). In each case further, longer Cl···H−O contacts exist. A similar layer structure was recently reported by Gandara et al. for $[Yb_4(OH)_{10}(H_2O)_4]$AQDS and $[Y_4(OH)_{10}(H_2O)_4]$NDS (AQDS, 2,6-anthraquinonedisulfonate; NDS, 2,6-naphthalenedisulfonate).[40] The layer structure reported here differs from that reported previously because of the lower hydration level of the chloride intercalate giving rise to less than nine-coordinate polyhedra, which alters the topology of the layer.

The "8.4 Å phase" crystallizes in the noncentrosymmetric orthorhomic space group $Pca2_1$ (No. 29) with an asymmetric unit of composition $Yb_2(OH)_5(H_2O)_{1.5}Cl$. Crystallographic details are given in Table 1 and the structure is illustrated in Figure 3. There are two independent Yb cations each coordinated by water and hydroxide, which bridges three Yb cations. Yb1 is coordinated by seven hydroxide ions and one fully occupied water molecule (O1w). Yb2 is coordinated by eight hydroxide ions and one-half occupied water molecule (O2w). In a way similar to that of the 8 Å phase, the hydroxide and Yb cations form a dense layer with composition $[Yb_2(OH)_5(H_2O)_{1.5}]^+$, but the thickness of this layer varies slightly. Yb1 polyhedra share edges to form rows

(40) Gandara, F.; Perles, J.; Snejko, N.; Iglesias, M.; Gomez-Lor, B.; Gutierrez-Puebla, E.; Monge, M. A. *Angew. Chem., Int. Ed.* **2006**, *45*, 7998.

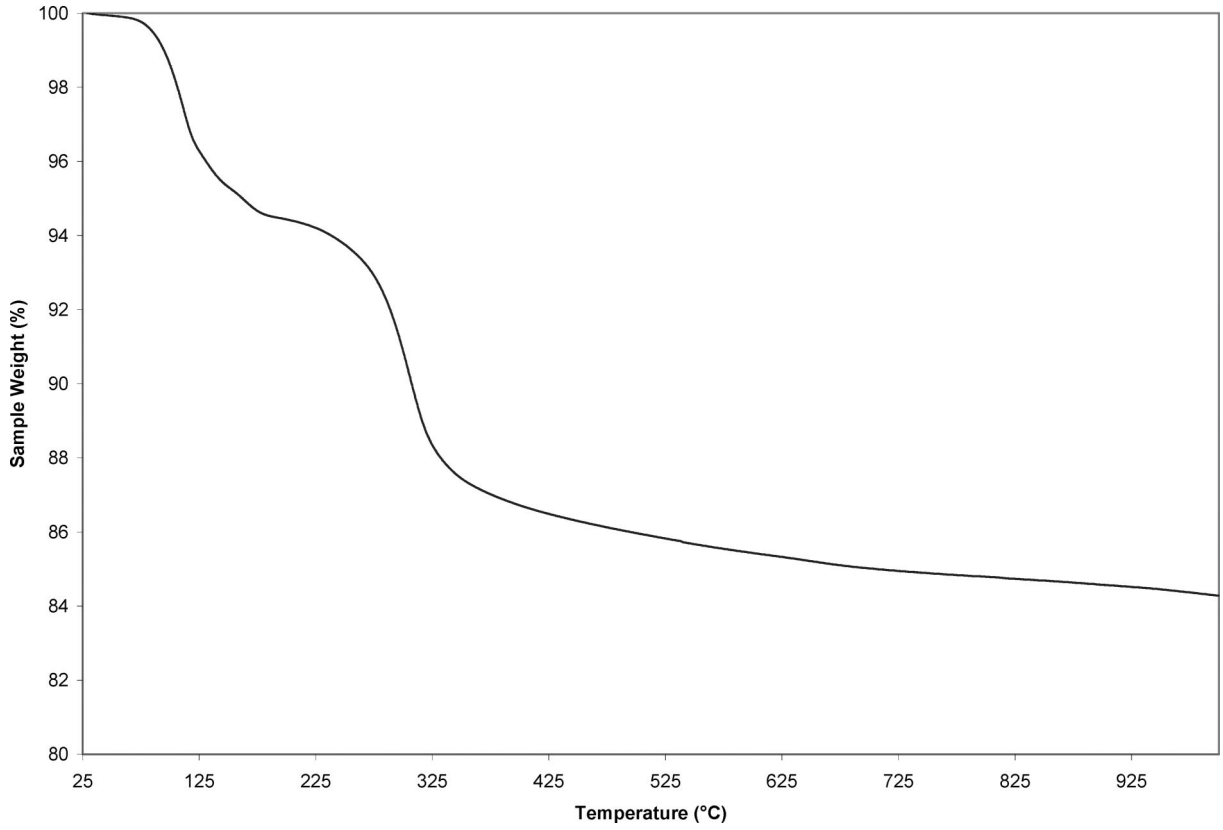

Figure 4. TGA trace for $Er_2(OH)_5Cl\cdot 1.5H_2O$ showing mass losses of 5.6% below 200 °C and a further mass loss of 9.0% by 600 °C.

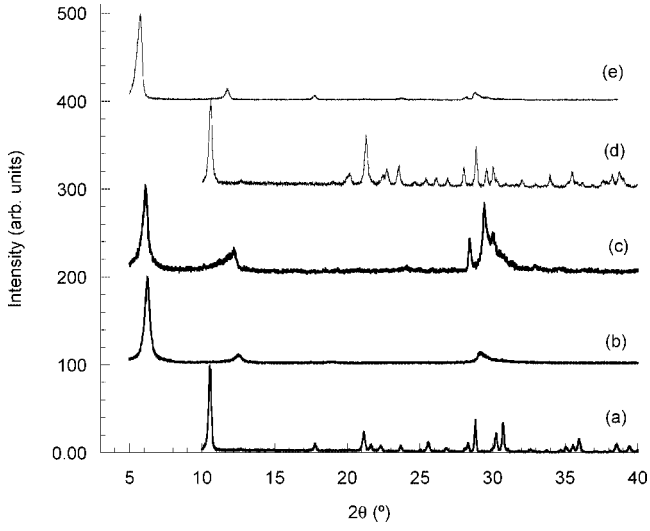

Figure 5. Powder X-ray diffraction patterns of (a) $Er_2(OH)_5Cl\cdot 1.5H_2O$, (b) the anion exchange derivative $Er_2(OH)_5(o\text{-}C_8H_4O_4)_{0.5}\cdot 1.5H_2O$, (c) $Yb_2(OH)_5(o\text{-}C_8H_4O_4)_{0.5}\cdot 1.5H_2O$ showing a single phase following anion exchange, (d) $Y_2(OH)_5Br\cdot 1.5H_2O$, and (e) the anion exchange derivative $Y_2(OH)_5(o\text{-}C_8H_4O_4)_{0.5}\cdot 1.5H_2O$.

where the layer is two polyhedra thick, but Yb2 polyhedra share faces to form rows where the layer is one polyhedron thick. When the structure is viewed down *c* an ordered arrangement of water in three-quarters of the rows, similar to the 8 Å phase, can be seen. The middle row of each block of three contains only Yb2 and to these is bound half-occupied water. One symmetry independent chloride ion is located between the layers and resides within a tight hydrogen bonding pocket shaped like a distorted octahedron formed from three hydroxide anions and three bound water molecules in a fac arrangement. One Cl···O distance is rather short (2.70 Å), signifying a strong hydrogen bond, while the others lie in the range 3.03−3.25 Å. Adjacent layers overlie and are related by a unit translation along *b* (interlayer distance 8.3930(13) Å) as shown in Figure 3a.

Table 2. Characterizing data for the New Lanthanide Hydroxyhalides, $Ln_2(OH)_5\cdot 1.5H_2O$

Ln, X	composition	interlayer separation (Å)	elemental analysis obsd (%)	elemental analysis calcd (%)
Y, Cl	$Y_2(OH)_5Cl\cdot 1.5H_2O$	8.37	Y (53.74) H (2.40)	Y (54.66) H (2.48)
Dy, Cl	$Dy_2(OH)_5Cl\cdot 1.5H_2O$	8.41	Dy (68.46) H (1.61)	Dy (68.78) H (1.71)
Er, Cl	$Er_2(OH)_5Cl\cdot 1.5H_2O$	8.39	Er (69.40) H (1.55)	Er (73.63) H (1.67)
Yb, Cl	$Yb_2(OH)_5Cl\cdot 1.5H_2O$	8.42, 8.00	Yb (69.88) H (1.53)	Yb (70.11) H (1.63)
Y, Br	$Y_2(OH)_5Br\cdot 1.5H_2O$	8.35	Y (47.26) H (2.11)	Y (48.09) H (2.18)
Yb, Br	$Yb_2(OH)_5Br\cdot 1.5H_2O$	8.33, 8.77	Yb (64.20) H (1.42)	Yb (64.32) H (1.50)

The layers in the 8 Å and 8.4 Å phases are similar but differ because of slight changes in the orientation of the polyhedra within the layer and hence their thickness. The basic motif is very similar but the presence of disordered water (O2w) in the 8.4 Å phase leads to local differences. In neither crystal structure is there evidence for unbound water located between the layers. The use of PLATON suggests that there are no solvent accessible voids in either structure.[41]

The hydrothermal syntheses with Y, Dy, and Er yielded the 8.4 Å phase with no evidence in the powder X-ray diffraction patterns for the formation of the 8.0 Å polymorph

Table 3. Characterizing Data for the Anion Exchange Derivatives, $Er_2(OH)_5(guest)_{0.5}\cdot 1.5H_2O$

guest	composition	interlayer separation (Å)	elemental analysis	
			obsd (%)	calcd (%)
succinate	$Er_2(OH)_5(C_4H_4O_4)_{0.5}\cdot 1.5H_2O$	11.72	Er (66.08) C (4.75) H (1.96)	Er (66.29) C (4.76) H (2.00)
maleate	$Er_2(OH)_5(cis\text{-}C_4H_2O_4)_{0.5}\cdot 1.5H_2O$	10.22	Er (66.13) C (4.87) H (1.74)	Er (66.42) C (4.77) H (1.80)
phthalate	$Er_2(OH)_5(o\text{-}C_8H_4O_4)_{0.5}\cdot 1.5H_2O$	14.09	Er (62.89) C (9.22) H (1.97)	Er (63.28) C (9.09) H (1.91)
terephthalate	$Er_2(OH)_5(p\text{-}C_8H_4O_4)_{0.5}\cdot 1.5H_2O$	12.95	Er (63.00) C (8.81) H (1.81)	Er (63.28) C (9.09) H (1.91)

(see Figure 5a and the Supporting Information). Further characterization of these materials by TGA and elemental analysis confirmed their composition and the analytical data are summarized in Table 2. The TGA data are given in Figure 4 for $Er_2(OH)_5Cl\cdot 1.5H_2O$, from which it can be seen that there is a mass loss of 5.5% (calculated mass loss for $Er_2(OH)_5Cl\cdot 1.5H_2O$ is 5.6%) below 200 °C corresponding to the removal of the bound water and a further mass loss of 9.0% (9.3%) by 600 °C resulting from the decomposition of the hydroxide layers. No significant decomposition steps are observed above this temperature and powder X-ray diffraction of the residual material revealed it to be a mixture of Er_2O_3 and ErOCl. FTIR spectra of the materials (see the Supporting Information) were also recorded and show a band at approximately 1650 cm^{-1} due to the bending vibration of water and O−H stretches centered around 3500 cm^{-1}.

Hydrothermal syntheses using $LnBr_3\cdot nH_2O$ (Ln = Y, Yb) rather than $LnCl_3\cdot nH_2O$ yielded the analogous lanthanide hydroxybromide phases, $Ln_2(OH)_5Br\cdot 1.5H_2O$. As was the case with the chloride materials the Yb sample is biphasic with interlayer separations of 8.33 and 8.77 Å. This increase in the interlayer separation on going from chloride to bromide is consistent with the larger size of the bromide anion and is comparable to the difference which has been observed previously with LDHs.[13] Notably, when bromide is employed the Y phase forms the monoclinic structure (8 Å phase) with layer separation 8.3 Å (Figure 5d), but is found as the orthorhombic (8.4 Å) phase when chloride is the counter-anion. This suggests there is a subtle interplay between the size of the cation (hence layer thickness) and the hydrogen bonding of the guest anion to adjacent layers. The characterizing data for these materials is included in Table 2 and in the Supporting Information.

Following the synthesis of new layered hydroxyhalides, their anion exchange chemistry was investigated by reaction with dicarboxylate salts. Successful reactions were observed for the $Ln_2(OH)_5X\cdot 1.5H_2O$ (X = Cl, Br; Ln = Y, Dy, Er, Yb) phases but not for the $Ln(OH)_2Cl$ materials. Powder X-ray diffraction and chemical analysis data demonstrate that $Er_2(OH)_5Cl\cdot 1.5H_2O$ undergoes complete exchange at room temperature. Diffraction peaks at *d*-spacings characteristic of the initial layer separation were completely replaced by others of longer *d*-spacing indicative of guest uptake, with the maleate, phthalate, terephthalate, and succinate anions forming materials with the composition $Er_2(OH)_5(guest)_{0.5}\cdot 1.5H_2O$. Typical powder X-ray diffraction patterns of the anion exchange products of $Er_2(OH)_5Cl\cdot 1.5H_2O$ are shown in Figure 5 and the characterizing data given in Table 3. The corresponding data on the anion exchange products of the other host lattices is included in the Supporting Information. The interlayer separations observed for the aromatic carboxylates are comparable to those seen for the dicarboxylate interca-

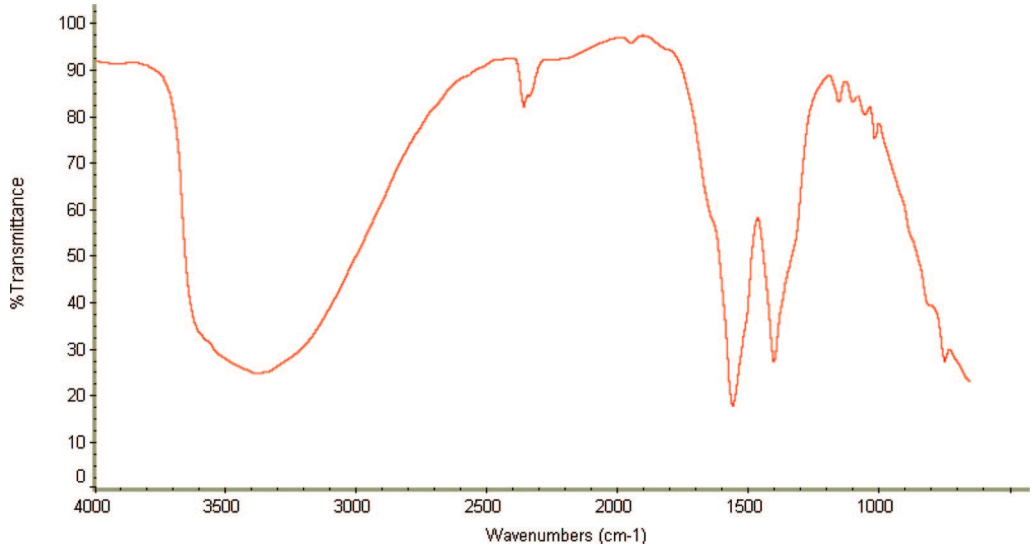

Figure 6. FTIR spectrum of $Y_2(OH)_5(o\text{-}C_8H_4O_4)_{0.5}\cdot 1.5H_2O$.

lates prepared from the lanthanide hydroxynitrates while those of succinate and maleate are larger.[25] In general the interlayer separations are smaller than those seen for the LDHs where succinate typically gives rise to a spacing of 12.1 Å compared to the 10.7 Å for $Er_2(OH)_5(C_4H_4O_4)_{0.5} \cdot 1.5H_2O$ observed in this study.[42,43] In the case of the biphasic $Yb_2(OH)_5Cl \cdot 1.5H_2O$ system both phases were observed to undergo anion exchange with succinate, maleate, phthalate, and terephthalate forming a single product as can be seen in Figure 5c for $Yb_2(OH)_5(o\text{-}C_8H_4O_4)_{0.5} \cdot 1.5H_2O$. The fact that a single phase results from these anion exchange reactions reflects the polymorphic relationship between the two $Yb_2(OH)_5Cl \cdot 1.5H_2O$ phases. The ease of anion exchange in these materials is comparable to that seen in the $Ln_2(OH)_5NO_3 \cdot 1.5H_2O$ compounds and occurs more readily than for $La(OH)_2NO_3$, which required prolonged heating at 60 °C to bring about complete exchange.[25,33] These observations are consistent with the different coordination environments of the intercalated anions in these systems with the more forcing conditions required when the anion is directly coordinated to the metal cation in the layer.

Further characterization of the anion exchange derivatives was achieved by FTIR spectroscopy as shown in Figure 6 for $Y_2(OH)_5(o\text{-}C_8H_4O_4)_{0.5} \cdot 1.5H_2O$. Strong bands in the spectrum at approximately 1550 and 1400 cm^{-1} correspond to the symmetric and asymmetric stretches, respectively, of the carboxylate groups of the intercalated phthalate anion. The positions of these bands are consistent with observations made on other layered hydroxide systems intercalated with carboxylate anions.[25,44]

Similar results were observed for the hydroxybromide materials with room temperature anion exchange reactions being observed with the maleate, phthalate, terephthalate and succinate anions. A comparison of the anion exchange products from the chloride and bromide hosts can be made from Figure 5c and 5e, from which it can be seen that the same material is formed in each case, suggesting that the layer structure is the same in both the lanthanide hydroxychlorides and hydroxybromides.

Conclusions

New lanthanide hydroxyhalides, $Ln_2(OH)_5X \cdot 1.5H_2O$ (X = Cl, Br; Ln = Y, Dy, Er, Yb), have been synthesized hydrothermally. The majority of the materials were obtained as pure phases; however, the Yb materials were always biphasic. Single-crystal diffraction studies showed that one Yb polymorph is monoclinic while the other is orthorhombic and it is the latter that is formed by the other lanthanide hydroxychloride hosts. In both cases the layer composition is the same and both contain eight and nine coordinate Yb sites with bridging hydroxide groups and coordinated water molecules. The structures differ in the arrangement of layers and presence of water projecting from the layer which leads to different hydrogen bonding to guest anions. These structures are the first determined for the $m = 1$ members of the $Ln_2(OH)_{6-m}(A)_m \cdot nH_2O$ family of intercalation hosts. $Yb_2(OH)_5Br \cdot 1.5H_2O$ is also biphasic displaying larger interlayer separations of 8.33 and 8.77 Å although in this case $Y_2(OH)_5Br \cdot 1.5H_2O$ forms the phase with the smaller interlayer spacing. All of the hydroxyhalide intercalation hosts have been found to undergo facile anion exchange reactions at room temperature with a range of organic dicarboxylate anions.

Acknowledgment. We thank EPSRC for funding under EP/D060664/1 and STFC for access to Station 9.8 of the U.K. SRS, Daresbury Laboratory. A.M.F. thanks the Royal Society for a University Research Fellowship.

Supporting Information Available: Further details of the crystal structure investigations may be obtained from Fachinformationszentrum Karlsruhe, 76344 Eggenstein-Leopoldshafen, Germany (fax: (+49)7247−808−666; e-mail: crysdata@fiz-karlsruhe.de, http://www.fiz-karlsruhe.de/request_for_deposited_data.html) on quoting the appropriate CSD number: 8 Å phase, 419743; 8.4 Å, phase 419745. Further details of the structural refinements, crystal structures, and additional characterizing data (powder XRD, FTIR, and elemental analysis) on both the host lattices and anion exchange derivatives are provided (PDF and CIF). This material is available free of charge via the Internet at http://pubs.acs.org.

CM802301A

(41) Speck, A. L. *J. Appl. Crystallogr.* **2003**, *36*, 7.
(42) Meyn, M.; Beneke, K.; Lagaly, G. *Inorg. Chem.* **1990**, *29*, 5201–5207.
(43) Williams, G. R.; Dunbar, T. G.; Beer, A. J.; Fogg, A. M.; O'Hare, D. *J. Mater. Chem.* **2006**, *16*, 1222.
(44) Li, F.; Zhang, F. H.; Evans, D. G.; Forano, C.; Duan, X. *Thermochim. Acta* **2004**, *424*, 15.